Vision Res. Vol. 27, No. 11, pp. 1915–1924, 1987
Printed in Great Britain.

0042-6989/87 $3.00 + 0.00

THE PHYSICAL LIMITS OF GRATING VISIBILITY

MARTIN S. BANKS,[1] WILSON S. GEISLER[2] and PATRICK J. BENNETT[1]

[1]School of Optometry and Department of Psychology, University of California, Berkeley, CA 94720 and
[2]Department of Psychology, University of Texas, Austin, TX 78712, U.S.A.

(*Received* 19 *August* 1986; *in revised form* 24 *April* 1987)

Abstract—We examined the extent to which pre-neural factors constrain the detectability of sinusoidal gratings of different spatial frequencies and luminances. Contrast sensitivity functions were measured in two observers for foveally-presented grating patches. Spatial extent of the patches was inversely proportional to grating frequency. The observers' contrast sensitivity functions were then compared to the performance of an ideal discriminator (Geisler, 1984) which incorporated the effects of quantal fluctuations, optical transfer, ocular media transmittance, and the aperture, quantum efficiency, and spatial distribution of foveal photoreceptors. The sensitivity of the ideal discriminator was roughly 20-fold greater than that of the human observers, but the shapes of the ideal and human CSFs were quite similar from 5 to 40 c/deg and from 3.4 to 340 cd/m^2. The similarity of shapes demonstrates that the high-frequency rolloff of the foveal CSF for gratings with a fixed number of cycles can be explained by the operation of pre-neural factors alone. Previous research has shown that grating summation area is inversely proportional to the square of spatial frequency. Thus, for gratings with fixed spatial extent the high-frequency rolloff can be explained by the pre-neural factors plus variations in grating summation area. These conclusions imply in turn that the neural transfer function is much flatter than previously thought and that private line connections from foveal photoreceptors to higher visual centers are common.

Contrast sensitivity Optics Ideal observer Receptor lattice Fovea

INTRODUCTION

A fundamental question is visual science is how optical and neural factors combine to determine visual performance. Here we consider how such factors limit the visibility of sinusiodal gratings presented to the fovea at photopic luminances. Sinusiodal gratings were chosen because, as implied by Fourier's theorem, any two-dimensional, achromatic stimulus can be represented by the combination of gratings of different spatial frequencies, contrasts, orientations, and phases. Thus, an understanding of factors constraining grating visibility should provide useful insights into how those factors influence visual performance in general.

It is well-known that the function relating the spatial frequency and detectability of a grating—the contrast sensitivity function (CSF)—is bandpass with peak sensitivity at 3–6 c/deg. Several investigators have examined factors that determine the CSF for foveal vision (e.g. Campbell and Green, 1965; Kelly, 1977; Westheimer, 1960; Williams, 1985a,b). One factor is defocus produced by the eye's optics. The effects of optical defocus can be virtually eliminated by using laser interferometry to generate sinusiodal gratings directly on the retina. Contrast sensitivity is higher for interference gratings than for gratings viewed conventionally, but in both situations, the CSF is bandpass with sensitivity falling monotonically from approximately 5 c/deg to the highest spatial frequency visible. It has been argued (Campbell and Green, 1965; Campbell and Gubisch, 1966; Snyder and Srinivasan, 1979; Westheimer, 1972) that these interferometric CSFs represent the differential sensitivity of the retina and visual brain to spatial frequency (or stated another way, they represent the "neural transfer function"). By this reasoning, the neural transfer function is bandpass with sensitivity falling substantially from intermediate to high spatial frequencies. Snyder and Srinivasan (1979), for example, argued that the neural transfer at 40 c/deg is only about 9% of the transfer at 5 c/deg.

The conclusion that the neural transfer function declines markedly from medium to high frequencies may be premature because the interferometry experiments reveal only the effects of optical defocus. Assuredly, additional pre-neural factors affect grating visibility. These include quantal fluctuations in the stimulus, transmittance of the ocular media, and the aperture, quantum efficiency, and spatial distri-

bution of foveal photoreceptors. The question we raise is: To what extent do these pre-neural factors constrain the detectability of gratings of different spatial frequencies and luminances?

Geisler (1984) and Geisler and Davila (1985) have developed an ideal discriminator for spatial vision that allows one to assess the contributions of pre-neural factors to the detection and discrimination of spatial stimuli. The ideal discriminator uses an optimal decision rule to discriminate stimuli on the basis of different effective quantum catches among photoreceptors. In other words, the discriminator performs as an ideal machine would if it had the optics and photoreceptors (up the point of isomerization) of the human fovea.

Others have used ideal observer analyses to determine the efficiency of human observers in grating detection tasks. Watson *et al.* (1983), for instance, evaluated human efficiency in detecting Gabor patches by comparing real performance to that of an ideal detector. Their computations of ideal performance were based on the stimulus at the cornea, so their approach revealved the efficiency of the visual system as a whole. Our approach is different. We compute ideal performance based on the quantum catches among photoreceptors in order to determine the efficiency of the rest of the visual system.

In this paper we compare ideal and human observers' performance on the same tasks with the same foveally-presented stimuli. Any differences between ideal and human performance should delineate the contributions of later neural factors. We emphasize the high-frequency slope of the CSF, from 5 to 40 c/deg, because the visibility of lower spatial frequencies is clearly influenced by retinal network interactions (e.g. Kelly, 1977) that are not incorporated in the ideal discriminator.

METHODS

To allow the comparison of neural efficiency across spatial frequency, real and ideal observers should have acess to the same stimulus information. To ensure this, we used stimuli whose spatial extent matched the spatial summating properties of real observers' detecting mechanisms. Several experiments have shown that the detectability of a grating increases with the number of cycles presented up to a critical number (Howell and Hess, 1978; Koenderink *et al.*, 1978; Robson and Graham, 1981). Once the critical number is reached, threshold is almost independent of number of cycles. The critical number of cycles does not appear to vary from one spatial frequency to the next (except at very low frequencies). Moreover, the critical height of a patch of vertical grating is the same as the critical width for a wide range of frequencies (Howell and Hess, 1978). These observations imply that real observers benefit from the addition of more cycles (or from lengthening the cycles), but only up to a point. The critical width and height are inversely proportional to spatial frequency. The ideal observer, in contrast, can effectively utilize information across the entire grating patch, no matter how large the patch is. Consequently, we used gratings whose extent was inversely proportional to spatial frequency. This in effect reduced the contribution of spatial summation to the shape of real and ideal CSFs. The targets were cosinusoidal gratings damped vertically and horizontally by half-cosine. The grating patches were presented in an otherwise uniform field of the same space-average luminance. The half-cosine window was adjusted to encompass 7.5 cycles of the grating target for all conditions, so the bandwidth of the targets was always ± 0.18 octaves. The space-average luminance of the stimuli was 340, 34, or 3.4 cd/m^2.

The stimuli were presented on a Joyce Electronics display with P4 phosphor. To ensure that the spatial transfer function of the display did not affect contrast thresholds, we fixed the period of the grating on the display and varied spatial frequency by changing viewing distance. Initially the viewing distances were 0.7, 0.99, 1.4, 1.98, 2.8, 3.96, and 5.6 m, yielding spatial frequencies of 5, 7, 10, 14, 20, 28, and 40 c/deg. However, preliminary measurements indicated that the phosphor grain of the display elevated contrast thresholds at the two nearest distances. This masking effect was eliminated by increasing those distances by a factor of four.

Two emmetropic observers viewed the stimuli monocularly through an artificial pupil of 2 mm. Head position was stabilized with a bite bar and head rest. Accommodation was paralyzed with 1% cyclopentolate, and both observers were optically corrected at each viewing distance. The appropriate correction was found by varying the power of ophthalmic lenses, placed as close to the cornea as possible, in 0.12 D steps. We chose the lens that maximized contrast sensitivity. Any residual errors in optical correction are unlikely to have affected our findings because with a 2 mm pupil the dioptric

change needed to decrease contrast sensitivity from its peak value is about 0.5 D at 9 c/deg and 0.25 D at 30 c/deg (Green and Campbell, 1965).

Contrast thresholds were estimated with a 2-interval, forced-choice procedure in which contrast was varied according to a 2-down/1-up staircase rule. Each trial was initiated by the observer and consisted of two 100-msec intervals marked by tones. The no-signal interval contained a uniform patch of the same space-average luminance as the target grating. Auditory feedback indicating the accuracy of the observer's response was given after each trial. Threshold was defined as the geometric mean of the final 6 staircase reversals. Each data point reported here is the geometric mean of at least 3 staircases.

RESULTS

We now consider the ideal discriminator's performance for our experimental conditions. (The reader who is unfamiliar with calculations of ideal performance in tasks like ours can refer to Geisler, 1984, Geisler and Davila, 1985, Van Trees, 1968, and Watson *et al.*, 1983). The parameters used here are the same as those used by Geisler (1984). The number of photons absorbed by each photoreceptor was Poisson distributed. The point spread function representing optical transfer was derived from Campbell and Gubisch (1966). Specifically, Campbell and Gubisch's line spread function for a 2 mm pupil was approximated by the sum of two Gaussian functions. The point spread function was then obtained from the smooth double Gaussian function by assuming that the optics are isotropic. The receptor lattice was packed in a triangular array such that the internodal distance equaled the 0.6 min diameter of foveal cones. The predictions are not altered when models of actual receptor lattices are used (Perry and Cowey, 1985). The receptor aperture was assumed to be 0.6 min, the intercone distance. We also followed Geisler's assumptions about ocular media transmittance and receptor quantum efficiency.

The effects of small eye movements were examined by comparing thresholds with some position uncertainty to those with no uncertainty. The standard deviation of eye position under good fixation conditions is about 4 min (Steinman, 1965; Rattle, 1969). If the visual system does not encode these eye position variations, they would introduce position uncertainty and, consequently, some loss of sensitivity. The potential effects of such uncertainty were examined by applying the ideal observer described in Geisler and Davila (1985) to the stimuli of the present experiment. The sensitivity loss due to position uncertainty varies only slightly with spatial frequency. From 10 to 40 c/deg an uncertainty of ± 4 min decreases contrast sensitivity by about 0.2 log units. Above 40 c/deg the effect is slightly larger, reaching 0.3 log units at 60 c/deg. The effect decreases at low spatial frequencies, reaching 0.1 log units just below 5 c/deg. Thus, it seems safe to conclude that any information loss at the retina due to small eye movements during fixation has little effect on the shape of the CSF over the range of spatial frequencies considered here.

Figure 1 illustrates what happens to the grating and uniform patches as they pass through the early processing stages. The grating patch is a damped 20 c/deg cosinusoid. The top panels illustrate samples of the stimuli at the cornea. The randomness of the curves represents quantal fluctuations. The middle panels show the stimuli after blurring by the optics of the eye. The bottom panels show the pattern of photon absorptions among the photoreceptors; each element of the histograms represents the photon catch of a single photoreceptor. By the level of photoreceptor activation, the spatial distributions of intensity have been noticeably degraded.

The ideal discriminator applies a maximum likelihood decision rule at the level of photon capture in the photoreceptors (the bottom panel in Fig. 1). The rule involves computing a particular weighted sum across the receptors for each interval. The interval yielding the larger sum is chosen as the one containing the grating. This maximum likelihood decision rule yields the best possible performance given the distorting effects of the earlier stages.

The contrast sensitivity functions of the ideal observer are displayed in Fig. 2. Different functions illustrate the contributions of various preneural factors. The highest broken line represents the performance of an ideal machine with no optical defocus and arbitrarily small and tightly packed photoreceptors. Space-average luminance is 340 cd/m^2 for this line. The contrast sensitivity values represent only the effects of quantal fluctuations in the stimulus, ocular media transmittance, and photoreceptor quantum efficiency. Media transmittance and receptor efficiency have a constant effect for all

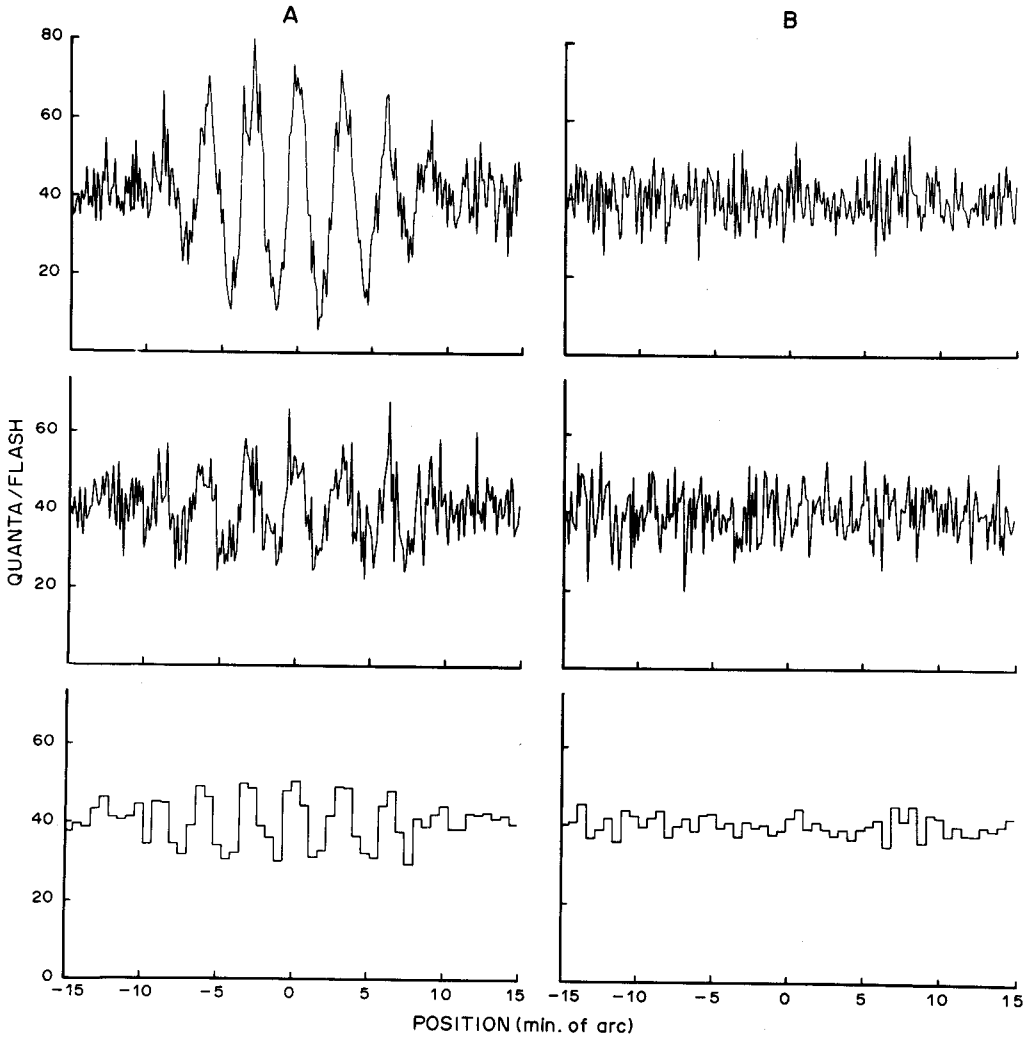

Fig. 1. Transmission through the pre-neural processes of a 20 c/deg cosinusoidal grating patch (A) and a uniform patch (B). The top panels illustrate samples of the stimuli at the cornea. The middle panels show the stimuli after blurring by the optics of the eye. The bottom panels show the pattern of photon absorptions in the photoreceptors. The actual model contained complete two-dimensional optics and a two-dimensional receptor lattice.

spatial frequencies, so quantal fluctuations are responsible for the inverse relation between sensitivity and spatial frequency, a point we expand below. The lower broken line represents performance with the effect of the receptor aperture added in. Finally, the highest solid line represents performance at 340 cd/m^2 with all pre-neural factors included; the difference between this curve and the one above it represents the contribution of optical defocus. The other solid lines represent the contrast sensitivities for 34 and 3.4 cd/m^2.

Quantal fluctuations are responsible for two properties of these curves: (1) the separations between the curves for different luminances, and (2) a significant portion of the high-frequency rolloff. The separations between the curves at different luminances are equal to the square root of the luminance ratios. This property is consistent with the familiar observation that ideal machines, limited by quantal fluctuations, exhibit a square root relation between threshold and background intensity (Barlow, 1958; Rose, 1942). The fraction of the high-frequency rolloff that is accounted for by quantal fluctuations is represented by the highest broken line. Recall that stimulus extent, and hence the square root of stimulus area, is inversely proportional to spatial frequency. Because noise-limited ideal machines exhibit a square root relation between threshold and stimulus area (Barlow, 1958), the effect of quantal fluctuations produces a line

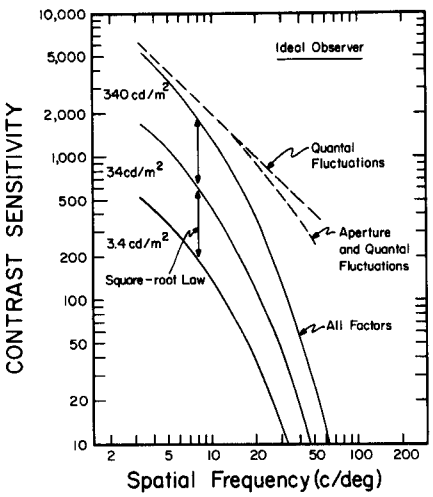

Fig. 2. Contrast sensitivity functions of the ideal discriminator. Contrast sensitivity, which is the reciprocal of contrast at detection threshold, is plotted against the spatial frequency of the grating targets. Different functions illustrate the contributions of various pre-neural factors. The highest broken line represents the performance of an ideal machine with no optical defocus and arbitrarily small and tightly packed photoreceptors. Space-average luminance is 340 cd/m². The contrast sensitivities represent only the effects of quantal fluctuations in the stimulus, ocular media transmittance, and photoreceptor quantum efficiency. The lower broken line represents performance with the receptor aperture effect added in. Finally, the highest solid line represents performance with all factors included; the difference between this curve and the one above it represents the contribution of optical defocus. The other solid lines represent the contrast sensitivities for 34 and 3.4 cd/m².

with a slope of −1 in this log–log plot. If stimulus extent had been fixed rather than inversely related to spatial frequency, the slope of the line would have been 0.

Of most interest is the comparison of ideal and human observers' performance. Figure 3 displays the contrast sensitivities for observers M.S.B. and P.J.B. for the three luminances tested. As is normally observed, contrast sensitivity declines monotonically for spatial frequencies above 5 c/deg, and sensitivity is greater for high than for low luminances. The CSFs are quite similar in shape to those reported previously (Howell and Hess, 1978; Robson and Graham, 1981; see Fig. 5).

As one would expect, the contrast sensitivity values of the two observers are substantially lower than those of the ideal discriminator. The question of greatest interest, however, is how changes in spatial frequency and luminance affect real and ideal performance. We examined this question by computing the ratio of the real observers' contrast threshold to the ideal discriminator's threshold for all of the spatial frequencies and luminances tested. The ratios are shown at the bottom of Fig. 3. In almost all cases, they were between 15:1 and 30:1, and they did not increase or decrease systematically with changes in spatial frequency or luminance. The similarity of these ratios across stimulus conditions can be illustrated by plotting ideal and real performance together. The average threshold ratio (real/ideal) was 21.5 for M.S.B. and 26.7 for P.J.B. The solid lines in the top section of Fig. 3 are not fits to the data, but rather are the CSFs of the ideal discriminator once shifted vertically by those amounts. The solid lines fit the experimental data rather well, which implies that space-average luminance and spatial frequency influence contrast sensitivity in the same fashion in human and ideal observers.

The real/ideal threshold ratios were rather high, but much smaller ratios can be obtained. For instance, we conducted a contrast discrimination experiment with grating patches of 7, 14, and 28 c/deg. The results for the 14 c/deg patch are illustrated in Fig. 4. The real/ideal threshold ratios fell to roughly 7:1 when the background contrast was at detection threshold. Even lower threshold ratios should be observed with smaller grating patches, although we have not yet confirmed this experimentally. Our reasoning is the following. The contrast sensitivity of the

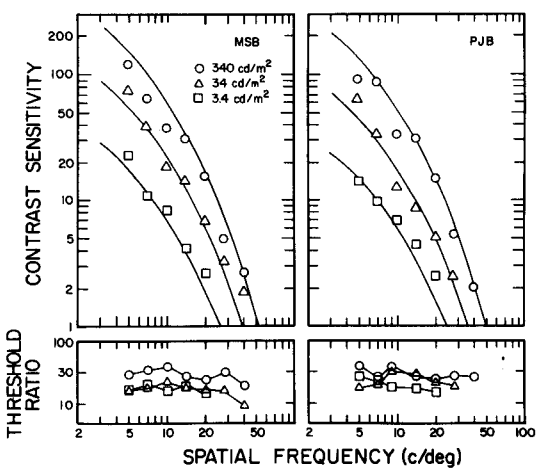

Fig. 3. Contrast sensitivity functions of observers M.S.B. and P.J.B. The upper panels plot contrast sensitivity as a function of spatial frequency for the three luminances tested. Each data point represents the mean of at least 3 staircases. The solid lines are the CSFs of the ideal discriminator, once shifted downward by 1.33 log units for M.S.B. and 1.43 log units for P.J.B. The lower panels plot threshold ratios as a function of spatial frequency. The ratios are the human observers' contrast thresholds divided by the ideal discriminator's thresholds.

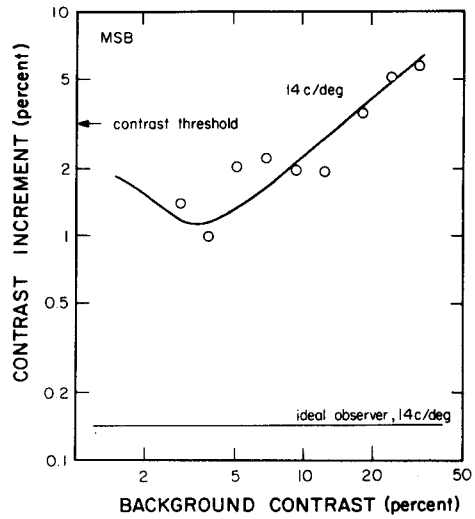

Fig. 4. Contrast discrimination functions for ideal observer and M.S.B. The contrast increment required for reliable discrimination is plotted as a function of background contrast. The target was a 14 c/deg grating patch. The contrast threshold for detecting the target is indicated by the arrow on the ordinate. The contrast discrimination function of the ideal discriminator for the same target is also displayed.

ideal discriminator is proportional to the square root of stimulus area. On the other hand, the contrast sensitivity of human observers is roughly proportional to the quarter root of stimulus area when fewer than 7 cycles are presented (Howell and Hess, 1978). One could, therefore, expect real/ideal threshold ratios of about 4:1 in contrast discrimination tasks for grating patches with only 2.5 cycles.

DISCUSSION

Relation to previous observations

The ideal discriminator incorporates all factors up to the point of effective quantum catch by the photoreceptors. Therefore, our results imply that later neural mechanisms signal spatial contrast, from 5 to 40 c/deg, equally reliably as a function of luminance (at least from 3.4 to 340 cd/m^2). Kelly (1977) and Van Nes and Bouman (1967) also observed that human and ideal observers are affected similarly by changes in stimulus luminance. Kelly reported that contrast sensitivity to medium and high spatial frequencies increased with the square root of retinal illuminance from 0.72 to 720 td. Above 720 td, contrast sensitivity approached constant values from one illuminance to another. The change from square root to constant behavior occurred earlier for medium than for high spatial frequencies. Our highest retinal illuminance was 1069 td. As one might expect from Kelly's observations, the largest deviations between ideal and human performance in the present experiment occurred at this illuminance for medium frequencies.

The similarity of the shapes of the ideal and real observers' CSFs implies that neural mechanisms signal spatial contrast equally reliably from 5 to 40 c/deg for gratings with a fixed number of cycles. This implication is rather surprising because it means that the differences in visibility among those spatial frequencies, when presented foveally, can be explained by pre-neural factors alone. Recall, however, that we controlled for the effect of spatial summation (a neural factor) by using grating patches with a fixed number of cycles. Thus, the reasonably accurate predictions of CSF shape by pre-neural factors suggest that spatial summation limited to a fixed number of cycles is the only important source of neural information loss affecting CSF shape. If this conclusion is correct, the shape of the ideal discriminator's CSF for fixed cycle gratings should match the shapes of previously reported CSFs, measured under appropriate conditions. The left panel of Fig. 5 compares human CSFs for gratings with fixed number of cycles with the ideal CSF. Although the high-frequency slopes of the human CSFs differ a bit from one another, the agreement between them and the ideal CSF is reasonably good. We also compared Williams' (1985b) interferometric CSFs to the ideal discriminator's CSF with the optical transfer function set to 1.0 (no optical defocus). Williams used 1–1.5 deg grating patches, so a sufficient number of cycles was present to allow the comparison from 10 to 60 c/deg. The right panel of Fig. 5 displays those functions. Again the agreement is rather good despite the variability among Williams' observers. Thus, the high-frequency slope of the ideal discriminator's CSF is at least consistent with previous observations. The congruence of the shapes of the real and ideal functions is also consistent with the hypothesis that spatial summation is the most important neural influence on CSF shape.

Re-examination of assumptions

The similarity of the high-frequency slopes of ideal and real observer's CSFs implies that neural efficiency is constant from medium to high spatial frequencies. Because this is an important result, the assumptions leading up to

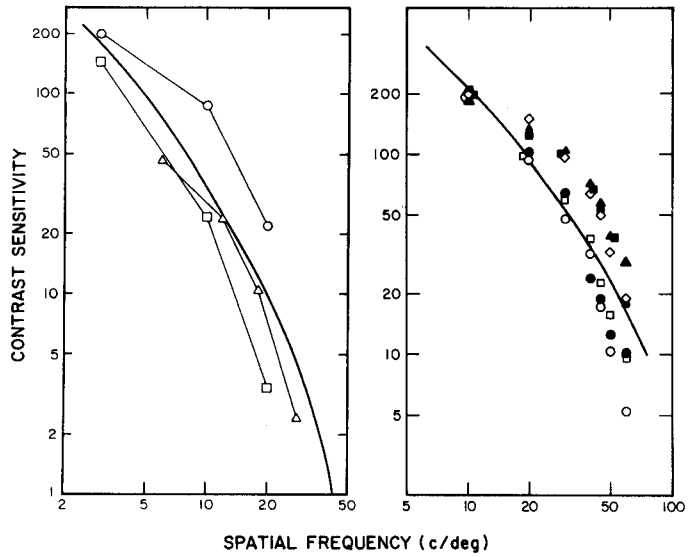

Fig. 5. Comparison of ideal discriminator's CSF and previously reported functions. The left panel displays foveal CSFs reported by Howell and Hess (1978), Koenderink *et al.* (1978), and Robson and Graham (1981). The Howell and Hess data are represented by the circles, the Koenderink *et al.* data by the squares, and the Robson and Graham data by the triangles. The ideal discriminator's CSF, with all pre-neural factors included, is represented by the heavy solid line. The line has been shifted vertically to maximize fit. The right panel displays foveal, interferometric CSFs reported by Willams (1985b). The different symbols represent data points from different observers. The solid line represents the ideal discriminator's CSF with quantal fluctuations and receptor aperture included. The solid line has been shifted vertically to maximize fit.

it should be examined carefully. Figure 2 shows how three factors—quantal fluctuations, receptor aperture, and optical transfer–determine the slope of the ideal observer's high-frequency roll-off. Here we consider our assumptions about each of these factors in detail.

As illustrated in Fig. 2, quantal fluctuations alone produce a line with a slope of -1 in log–log contrast sensitivity plots. We noted earlier that this inverse relation between contrast sensitivity and spatial frequecy is a consequence of using grating patches whose vertical and horizontal extents are inversely proportional to spatial frequency: ideal machines, limited by stimulus noise, exhibit a square root relation between sensitivity and target area and, therefore, a linear relation between sensitivity and target extent. Presumably, the close correspondence we report between ideal and real performance is only observed when target extent and spatial frequency are inversely related. Our reasoning is the following. The ideal discriminator can effectively utilize information across the entire grating patch. For gratings of fixed extent, the number of quanta relevant to detecting the grating would be similar from one spatial frequency to the next. Therefore, the effect of quantal fluctuations alone (the top curve in Fig. 2) would be nil. Real observers, on the other hand, do not benefit from the addition of more than 7–10 grating cycles (Howell and Hess, 1978). So real observers, to the extent that their performance is limited by quantal fluctuations, would still exhibit the inverse relation between sensitivity and spatial frequency for frequencies high enough to provide more than 7–10 cycles. Thus, if we had presented large targets of fixed extent, the high-frequency slope of the ideal CSF would have been much shallower than that of the real CSFs.

Next we examine our assumptions about the eye's optical transfer function. The function we used is based on Campbell and Gubisch's (1966) ophthalmoscopic measurements of line spread functions. Several sorts of measurement error in this double-pass technique (inexact focus of the line image, forward retinal scattering, etc.) can degrade estimates of optical transfer. Thus, one should consider the possibility that the optical transfer estimates of Campbell and Gubisch are too low. Their estimates are probably reasonably accurate for two reasons. (1) They are reasonably consistent with calculations of optical transfer. For example, Van Meeteren (1974) has calculated an optical transfer function for white light that incorporates diffraction due to the

pupil, and chromatic and spherical aberrations. His transfer function for a 2 mm pupil is similar to Campbell and Gubisch's 2 mm function. The largest deviation is at 40 c/deg where van Meeteren's function is 0.3 log units higher, a point we discuss below. (2) Campbell and Gubish's transfer functions are roughly consistent with recent laser interferometric experiments. As noted by Campbell and Green (1965), one can estimate the eye's optical quality by comparing CSFs measured using interference fringes (which mostly avoid optical degradation) to CSFs measured conventionally. Campbell and Green's original comparison revealed optical transfer functions that were significantly higher than Campbell and Gubisch's functions (see Fig. 12, Campbell and Gubisch, 1966). Williams (1985b), however, has argued that Campbell and Green's interferometric data were contaminated by laser speckle; his measurements using a modified interferometer revealed higher contrast sensitivity. If one compares, in the manner of Campbell and Green, Williams' data (for example, observer D.G. in his Fig. 4) to conventional CSFs (observer D.G. in Fig. 5 of Campbell and Green), the resulting optical transfer functions are similar to those of Campbell and Gubisch. For these two reasons, it seems likely that the optical transfer functions we used to compute CSFs for the ideal observer are reasonably accurate.

It is interesting to note, by the way, that the agreement between ideal and real performance is actually increased when we adopt a slightly higher optical transfer at high spatial frequencies (such as van Meeteren's function). Thus, the evidence supporting our main conclusion—that neural efficiency is roughly constant from 5 to 40 c/deg—would be even more persuasive if somewhat higher optical transfer values were used.

Another factor influencing the shape of the ideal observer's CSF is the receptor aperture. As described earlier, we assumed a receptor aperture of 0.6 min, the inter-cone distance. The small attenuation due to an aperture of this diameter is illustrated by the separation between the top two broken curves in Fig. 2. Miller and Bernard (1983) and Williams (1985b) have presented anatomical and psychophysical evidence that the aperture of foveal cones is actually about 0.48 min, which is 80% of the inter-cone distance. If we adopt this value in computing the ideal observer's CSF, the attenuation due to the receptor aperture is decreased slightly. In other words, the high-frequency slope of the ideal CSF becomes slightly shallower. Nonetheless, reducing the receptor aperture from 0.6 to 0.48 min has little effect on the correspondence between real and ideal performance because the aperture effect is quite small to begin with.

Thus, the conclusion that the high-frequency slopes of real and ideal CSFs are similar seems appropriate; the similarity is not abolished when optical transfer and receptor aperture are varied by plausible amounts, and the strategy of presenting grating patches whose extent is inversely related to spatial frequency is appropriate for matching target extent to summation area.

Implications for neural mechanisms

We conclude that the neural transfer function is much flatter than previously thought. It is interesting to consider the sorts of neural mechanisms that are consistent with the observation of constant neural efficiency from 5 to 40 c/deg. Ideal performance exceeded real performance by 1.2–1.5 log units, so one needs to keep in mind that some loss of information occurs in neural processing. The gap between ideal and real performance can be explained in two ways. First, a similar neural process might be responsible for the information loss at different spatial frequencies. Some possibilities are: (1) a uniform multiplicative attenuation process such as a ratio of less than 1.0 for the number of pigment molecules bleached to the number of quanta absorbed; (2) position or frequency uncertainty (see Methods section); (3) a fixed cycle summation area less than 7.5 cycles; (4) a source of neural noise that is similar to Poisson noise and exists in all spatial frequency mechanisms; (5) an appropriate combination of nonlinear transducer and neural noise that is similar across spatial frequency mechanisms; or (6) some combination of the above. The alternative hypothesis is that different processes could be responsible for the loss at different frequencies. Although this hypothesis cannot be rejected, it is unparsimonious because it implies that different processes produce information loss of the same magnitude.

The observations of constant neural efficiency for fixed-cycle gratings implies that high-frequency mechanisms are as efficient as mid-frequency mechanisms. If the first hypothesis is correct (that a similar neural process is responsible for the information loss between ideal

and real performance at different spatial frequencies), our data can be used to infer the spatial properties of neural mechanisms involved in grating detection. We pursued this by further data analysis. The gratings in this experiment were vertically oriented, so our analysis was one-dimensional. The experimental data points in Fig. 3 were transformed to remove the effects of optical defocus and stimulus quantal fluctuations. The transformed data were nearly flat from 5 to 40 c/deg. We then fit smooth functions, intersecting the abscissa at different frequencies, through the data.* The inverse Fourier transforms of those functions yielded smooth functions with full widths at half height from 0.38 to 0.64 min. Those widths are similar to, or even smaller than, the diameter of a single foveal cone. Assuming that grating detection involves neurons from the retina to the striate cortex, this finding implies the presence of "private line" connections from foveal cones to the center mechanisms of bipolar and retinal ganglion cells (Boycott and Dowling, 1969; Polyak, 1941) and of similar connections from the retina to the geniculate and cortex. Stated more precisely, our observations suggest that the center mechanisms of bipolar, retinal ganglion, geniculate, and cortical cells that contribute to the detection of foveally-presented, high-frequency gratings are fed by one foveal cone only (or in the case of cortical cells, by a column of foveal cones). Our stimuli were vertically oriented, so this analysis has implications only for the horizontal dimension of geniculate and vertically-oriented cortical receptive fields. As described two paragraphs below, our observations do not imply that the center mechanisms of mid-frequency detectors are fed by single cones or columns of cones.

Although only one cone or cone column may innervate the center mechanisms of high-frequency geniculate and cortical cells, this does not mean that receptive field widths of less than 1 min should be observed in electrophysiological experiments. Even for singly innervated cells, the widths of center mechanisms measured electrophysiologically should be larger than the diameter of one cone (e.g. Derrington and Lennie, 1984) because, in addition to neural transfer, the receptive field reflects the contributions of quantal fluctuations, optical defocus, and receptor aperture. All of these factors would increase the spatial extent of receptive fields observed in electrophysiological experiments.

A simple model is consistent with the observation of constant neural efficiency from intermediate to high frequencies and with the private lines hypothesis. Kelly (1975) proposed that cortical receptive fields are constructed by summing inputs from retinal ganglion cells (actually columns of ganglion cells) at nearly regular spatial intervals. In Kelly's model, a cortical receptive field most responsive to 5 c/deg could be constructed by summing ganglion cells separated by roughly 12 min, and one most responsive to 40 c/deg by summing cells separated by 1.5 min. He claimed that the contrast sensitivity of these receptive fields would be determined by the Fourier transform of the ganglion cell's spatial receptive field. With some modifications, this model is consistent with our observation of constant neural efficiency from intermediate to high spatial frequencies. Suppose again that cortical receptive fields are created by summing retinal elements at nearly regular intervals, but now think of the elements as foveal cones connected to the cortex via intermediate retinal and geniculate neurons. The excitatory lobes of high-frequency cortical receptive fields could be constructed by summing single cones (or actually columns of cones) separated by 1.5 min and inhibitory lobes by summing, in opposite polarity, single cones (or columns) in between. Mid-frequency fields could be constructed by a similar scheme but several cones (or columns) would be summed with different weightings to create larger excitatory lobes at intervals of roughly 12 min and inhibitory lobes at similar intervals. If the number of excitatory and inhibitory lobes of these receptive fields were similar for mid- and high-frequency cells, this scheme would exhibit constant neural efficiency for gratings with fixed numbers of cycles. The scheme also has private line connections for high-frequency mechanisms.

We should reiterate that our conclusion concerning private line connections hinges on the

*The functions we used in this analysis were of the form $\sin(bf)/bf$, where f is spatial frequency and 1/b is the frequency of the first zero. The functions were set to zero above 1/b. We attempted to fit a family of these functions to the transformed data from 5 to 40 c/deg. When the value of 1/b was between 80 and 140 c/deg, the deviation between the function and the data points was always less than 0.3 log units. For lower and higher values of 1/b, the deviations were greater. We then computed the inverse Fourier transforms of the functions with acceptable fits.

assumption that similar neural processes cause information loss at different spatial frequencies. The other possibility is that different processes are involved at different frequencies. If that view is correct, our data would not allow us to infer the spatial properties of neural mechanisms involved in grating detection.

CONCLUSION

This research illustrates how the ideal discriminator can provide a rigorous baseline against which to gauge the performance of human observers. Using this approach, we have shown that the luminance and spatial-frequency dependence of intermediate- and high-frequency grating detection in the fovea can be explained by pre-neural factors plus variations in grating summation area alone. Of course, we are not proposing an explanation of absolute contrast sensitivity values in the middle to high spatial frequency range because the ideal and human performance differed by a substantial factor. Several models of post-receptor processing could account for the observed difference in absolute levels of performance. Our major observation is that post-receptor mechanisms produce a flat neural transfer function in the fovea. This observation significantly constrains the possible properties of such mechanisms.

Acknowledgements—This research was supported by NIH Research Grants HD-19927 to M.S.B. and EY-02688 to W.S.G. We thank Theodore Cohn, Russell DeValois, Dennis McFadden, and Christopher Tyler for comments on an earlier draft, and Clifton Schor for the use of his microprocessor. Send correspondence to: Martin S. Banks, School of Optometry, University of California, Berkeley CA 94720.

REFERENCES

Barlow H. B. (1958) Temporal and spatial summation in human vision at different background intensities. *J. Physiol, Lond.* **141,** 337–350.

Boycott B. B. and Dowling J. E. (1969) Organization of primate retina: Light microscopy. *Phil. Trans. R. Soc.* **B255,** 109–184.

Campbell F. W. and Green D. G. (1965) Optical and retinal factors affecting visual resolution. *J. Physiol, Lond.* **181,** 576–593.

Campbell F. W. and Gubisch R. W. (1966) Optical quality of the human eye. *J. Physiol, Lond.* **186,** 558–578.

Derrington A. M. and Lennie P. (1984) Spatial and temporal contrast sensitivity of neurones in lateral geniculate nucleus of macaque. *J. Physiol.* **357,** 219–240.

Geisler W. S. (1984) Physical limits of acuity and hyperacuity. *J. opt. Soc. Am.* **A1,** 775–782.

Geisler W. S. and Davila K. D. (1985) Ideal discriminators in spatial vision: Two point stimuli. *J. opt. Soc. Am.* **A2,** 1483–1492.

Green D. G. and Campbell F. W. (1965) Effect of focus on the visual response to a sinusoidally modulated spatial stimulus. *J. opt. Soc. Am.* **55,** 1154–1157.

Howell E. R. and Hess R. F. (1978) The functional area for summation to threshold for sinusoidal gratings. *Vision Res.* **18,** 369–374.

Kelly D. H. (1975) Spatial frequency selectivity in the retina. *Vision Res.* **15,** 665–672.

Kelly D. H. (1977) Visual contrast sensitivity. *Optica Acta* **24,** 107–129.

Koenderink J. J., Bouman M. A., Bueno de Mesquita A. E. and Slappendel S. (1978) Perimetry of contrast detection thresholds of moving spatial sine wave patterns. III. The target extent as a sensitivity controlling parameter. *J. opt. Soc. Am.* **68,** 854–860.

van Meeteren A. (1974) Calculations on the optical modulation transfer function of the human eye for white light. *Optica Acta* **21,** 395–412.

Miller W. H. and Bernard G. D. (1983) Averaging over the foveal receptor aperture curtails aliasing. *Vision Res.* **23,** 1365–1370.

Perry V. H. and Cowey A. (1985) The ganglion cell and cone distributions in the monkey's retina: Implications for central magnification factors. *Vision Res.* **25,** 1795–1810.

Polyak S. (1941) *The Retina.* Univ. of Chicago Press, Chicago.

Rattle J. D. (1969) Effect of target size on monocular fixation. *Optica Acta* **16,** 183–192.

Robson J. G. and Graham N. (1981) Probability summation and regional variation in contrast sensitivity across the visual field. *Vision Res.* **21,** 409–418.

Rose A. (1942) The relative sensitivities of television pick-up tubes, photographic film, and the human eye. *Proc. Inst. Radio Engrs* **30,** 293–300.

Snyder A. W. and Srinivasan M. V. (1979) Human psychophysics: functional interpretation for contrast sensitivity vs spatial frequency curve. *Biol. Cyberne.* **32,** 9–17.

Steinman R. M. (1965) Effect of target size, luminance and color on monocular fixation. *J. opt. Soc. Am.* **55,** 1158–1165.

Van Nes F. L. and Bouman M. A. (1967) Spatial modulation transfer in the human eye. *J. opt Soc. Am.* **57,** 401–406.

Van Trees H. L. (1968) *Detection, Estimation, and Modulation Theory.* Wiley, New York.

de Vries H. (1943) The quantum character of light and its bearing upon the threshold of vision, the differential sensitivity and visual acuity of the eye. *Physica* **10,** 553–564.

Watson A. B., Barlow H. B. and Robson J. G. (1983) What does the eye see best? *Nature, Lond.* **31,** 419–422.

Westheimer G. (1960) Modulation thresholds for sinusoidal light distributions on the retina. *J. Physiol, Lond.* **152,** 67–74.

Westheimer G. (1972) Visual acuity and spatial modulation thresholds. In *Handbook of Sensory Physiology* (Edited by Jameson D. and Hurvich L. M.). Springer, Berlin.

Williams D. R. (1985a) Aliasing in human foveal vision. *Vision Res.* **25,** 195–205.

Williams D. R. (1985b) Visibility of interference fringes near the resolution limit. *J. opt. Soc. Am.* **A2,** 1087–1093.